ESIC2024 Posted: 16/04/2024 DOI: 10.70082/esic/8.1.089

The Effect of Tailwater on the USBR Type III Stilling Basin Model

Gilang Idfi[1], Umboro Lasminto[2], Anak Agung Gde Kartika[2]

[1]Doctoral Program of Civil Engineering Department, Faculty of Civil, Planning and Geo-Engineering, Institut Teknologi Sepuluh Nopember (ITS), Indonesia
[2]Lecturer of Civil Engineering Department, Faculty of Civil, Planning and Geo-Engineering, Institut Teknologi Sepuluh Nopember (ITS), Indonesia
Email: gilang.idfi.ft@um.ac.id

Abstract

This study evaluates the impact of tailwater on the USBR Type III stilling pond model, which is often used to construct reservoirs with low hydrostatic pressure and small flow rates. The model includes channel blocks, barrier blocks, and end barriers to dampen energy, converting flow from supercritical to subcritical. Hydraulic characteristics, including potential jump types, pressure regimes, and forces on the barrier, are not considered. Any change in discharge during the test also changes the tailwater depth position. The purpose of this study was to determine the effects of tailwater conditions on water height (y1 and y2), pool length (Lj), Froude number (Fr), critical depth (yc), and energy dissipation effectiveness (ΔE). This study shows that the average energy dissipation ratio of USBR Type III Quiet Pool is 87.45% without the effect of Tailwater, with an efficiency rate of 12.55%. When exposed to Tailwater, the average energy dissipation ratio drops to 69.47%, resulting in an efficiency rate of 30.53%. The optimum stilling pond performance is affected by the presence of tailwater (Tw), which reduces the energy dissipation ratio. The depth of the tailwater aids in the dissipation that occurs. Technical abbreviations will be explained in the first use. The water level rise under tailwater conditions exceeds that without tailwater. This finding shows tail water's importance for height rise and flow conditions. Flow conditions with Froude Number (Fr2) values of 0.22 (<1) and Tw are classified as subcritical flow.

Keywords: USBR Type III, Tailwater, Stilling Basin, The Energy Dissipation.

The energy dissipators are one of the most important parts of the dam spillway [1], [2]. This building has the function of reducing the supercritical flow energy from the channel (chute way) into the subcritical flow, which is returned to the river [3], [4]. In the dissipation process, there is a hydraulic jump phenomenon, which indicates the dissipation process [5]. Problems that often occur are that energy absorbers need to work optimally [6], which often results in scouring problems in the geometry of the river, which is at the base and cliffs of the river [7]. One variety of energy dissipators is the USBR (United States Bureau of Reclamation) type,

whose energy dissipation principle is primarily attributed to friction or collisions between water molecules, leading to the circulation of water in the basin [8] [9]. Therefore, it is called a stilling basin-type energy dissipator [10]. In theory, USBR type III is appropriate for the following circumstances. [11]: 1) flow with low hydrostatic pressure (Pw < 60 m); 2) small discharge (specific discharge, q < 18.5 m3/s/m); and 3) Froude number at the end of chute greater than 4.50 [12].

Deng et al. confirm that this study aims to improve the flow pressure prototype for hydrostatic loads, while a related study that examines the statistics of fluctuation pressure in the lower basin due to hydrostatic loads around lateral expansion was conducted by Yan et al. [13]. The effects of channel expansion rate and flow conditions settle in the daily spectrum and dominance frequency. The pressure data refer to different Froude numbers ranging from 3.52 to 6.86 and channel expansion ratios ranging from 1.5 to 3.0 [14], providing a numerical simulation of the smallest B-jumps occurring in horizontal rectangular channels with a sudden decline. Prior to that, Altan-Sakarya and Tokyay [15]. Conducted a numerical simulation of an A-type jump occurring at a positive step. A literature review indicates that earlier investigations into forced hydraulic jumps significantly emphasize the tailwater depth downstream of the stilling basin. Under identical flow and jump conditions, the tailwater depth may vary due to its close dependence on the slope and cross-sectional characteristics of the river downstream of the basin.

Svoboda et al discovered that the basin exhibited effective performance at tailwater elevations significantly lower than those specified in the standard design of the baffle block [16]. The findings and the research that prompted the initial extension of the basin raised inquiries regarding the impact of improved energy dissipation on a stepped spillway on the stilling basin's effectiveness. Svoboda et al. also determined that the stilling basin's performance, influenced by tailwater, increased by 6-12%.

USBR type III with its baffle blocks was designed to accelerate and shorten the hydraulic jump by forcing the turbulent process to occur from the entering flow at the toe of chute [17], [18]. That hydraulic jumps can also be controlled or directed by the existence of end sill to complete the dissipation at downstream [19], [20], where the planning of the height is associated with the need for water flow depth downstream of the energy reducer (tailwater depth) [21], [22]. Previous research from Peterka suggests that the effectiveness of an energy dissipator is highly depend on the performance of the energy dissipator itself and depends on downstream water conditions (tailwater level) [23], [24]. The minimum water depth that must be available is 0.8 conjugate depth (y2) for USBR type III [25], If it is less than the minimum depth, then there is no dissipation effectiveness because of the jumps that occur out of the stilling basin [26], [27]. To preserve the river geometry's integrity, it is crucial to guarantee the occurrence of hydraulic jumps in the stilling basin [28], [29].

A physical model experiment was conducted in this study to determine the extent of tailwater's impact on energy dissipation in a USBR type III stilling basin. To assess effectiveness of dissipation, a scenario was first conducted without tailwater, and then compared with tailwater applied at the calculated conjugate depth (TW = y2). This study aims to determine the effect of tailwater conditions on water level at the toe of spillway and at tis conjugation (y1 and y2), basin length (Lj), froude number (Fr), critical depth (yc), and the effectiveness of energy dissipation (ΔE) using physical experimental.

Materials and Method

Hydraulic Jump

A hydraulic jump occurs when water transitions rapidly from supercritical flow to subcritical flow, resulting in a sudden rise in

water level and significant energy loss [30]. The beginning of the jump is marked by the formation of a turbulent vortex, which draws energy from the main flow and subsequently fragments into smaller parts downstream [31]. For supercritical flow in a horizontal rectangular channel [32], the flow velocity and height in the flow direction will be reduced due to the frictional resistance of the channel [33], resulting in the suppression of flow energy. The momentum principle can be used to deduce the nature of the downstream flow and the energy loss in the hydraulic jump as a function of the Froude number and upstream flow depth [34], as shown in Figure 1.

In hydraulic jump occurrence, the basic component that affects the energy calculation is the momentum equation:

$$P_1 - P_2 = \rho Q(v_1 - v_2) \qquad (1)$$

$$\left(\frac{1}{2}\rho g {y_1}^2 - \frac{1}{2}\rho g {y_2}^2\right) B = \rho v_1 v_2 (y_1 - y_2) \quad (2)$$

where P is resultant of hydrostatic pressure; ρ as the density of water (1 g/cm3); B is width of the channel where the value can be taken as 1 length unit; v1 and v2 are velocities before and after the jump respectively; y1 and y2 are the depths before and after the jump respectively; and g is gravitational constant (9,81 m2/s).

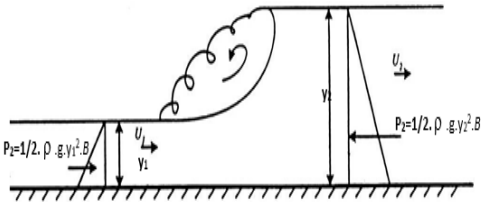

Figure 1. Momentum equation in hydraulic jump

While from continuity flow principle:

$$\frac{Q}{B} = q = v_1 y_1 = v_2 y_2 \qquad (3)$$

By combining those equations, then it is simplified as froude function of ratio of conjugate depth to pre-jump depth.

$$\frac{y_2}{y_1} = \frac{1}{2}\left(\sqrt{1 + 8{F_{r1}}^2} - 1\right) \quad (4)$$

The types of hydraulic jump are classified by Froude number occurred at the toe of chute as F_r1=v/√(gy_1). When the value of Fr is equal to one, there is no jump occurs. Bradley and Peterka [35] classified hydraulic jumps in four types.

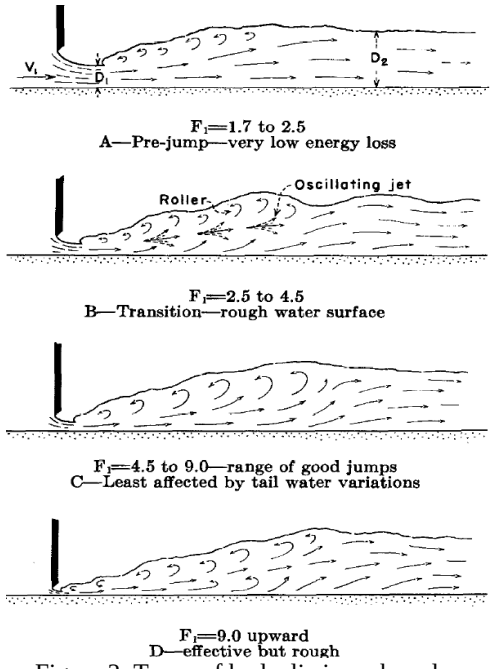

Figure 2. Types of hydaulic jump based on Froude number [36] (figures are taken from Kumcu and Ispir [12])

For Fr1 between 1.7 to 2.5; weak jump; pulsating waves form on the jump surface, while the water surface downstream remains smooth. The overall velocity remains uniform, with minimal energy loss. The ratio of y2 to y1 ranges from 2 to 3.1.

For Fr1 between 2.5 to 4.5; oscillating jump; oscillating jets are present at the base of the jump that move to and from the surface with no specific period. Each oscillation results in a large

irregular wave, causing extensive damage to the embankment. The y2/y1 ratio ranges from 3.1 to 5.9.

For Fr1 between 4.5 to 9; steady jump; the downstream flow surface edges undergo rolling, resulting in separation from the flow at the point of high burst velocity. Typically, both phenomena happen on the same vertical surface. The movements and surges that arise are not considerably impacted by the water depth at the bottom. The hydraulic jump is incredibly balanced, which is its best characteristic. Energy dissipation ranges from 45% to 70%. The y2/y1 ratio ranges from 5.9 to 12.

For Fr1 greater than 9; strong jump; the burst's high velocity separates the rolling waves from the springboard surface, creating downstream waves. Rough surfaces impact wave occurrence. Although rare, the jumping motion effectively attenuates up to 85% of energy. The y2/y1 ratio is greater than 12.

2.2 Experimental Setup

In this experiment, 10 discharge variations were applied without setting a barrier block as a tailwater regulator downstream of the flume so that the flow would directly slide into the catch basin downstream of the flume and flow back into the reservoir. Each model was tested to measure critical depth (yc), flow velocity along the spillway (v), flow depth (d1) before and after the hydraulic jump (d2), and hydraulic jump length (Lj).

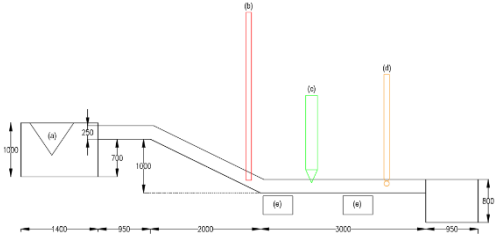

Figure 3. Schematic of measuring instrument placement (a) thompson measuring instruments / v-notch, (b) pitot pipes, (c) acoustic doppler velocimetry (ADV), (d) current meter, and (e) cameras

The measuring equipment is installed so that the flow does not sink, and the base of the sill is installed horizontally so that the incoming flow velocity becomes small. The placement of each measuring instrument can be seen in Figure 3. To simplify flow control and accuracy in data collection, measuring instruments are used to record discharge and velocity in the form of Thompson measuring instruments, pitot pipes, flow meters, Acoustic Doppler velocimetry (ADV) measuring instruments, and current meters. The measuring equipment used in this study is a sharp sill triangular weir, Thompson weir, or V-notch, with the length of each side of the triangle being 35 cm, as shown in Figure 4. The discharge used for this setup ranges from 6.124 to 30.546 l/s.

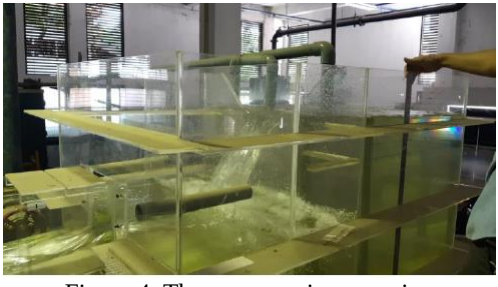

Figure 4. Thompson weir measuring instruments/ v-notch

2.3 USBR Type III Stilling Basin Design

As the results of all dischrages measurement, the rating curve is obtained as shown in Figure 5. For design purposes, a discharge value of 10.1 cm3/s was used and a head above the spillway of 14 cm was obtained. Flow depth (y1) and velocity (v1) before the jump and corresponding Froude number (Fr1) were calculated and gave the values of 1.44 cm, 351.58 cm/s, and 9,37 respectively. It shows that the values of Fr1 > 4.5, so USBR type III is suitable for the stilling basin design based on USBR type III design requirements.

Regarding to Peterka, where all the dissipators attributes depend on hydraulic parameter values at upstream basin, Figure 6

shows us the result of stilling basin design based on USBR type III standard. Chute block's height was designed based on entrance flow depth (y1), while the baffle piers and end sill were designed based on combination of both entrance flow depth (y1) and Froude number value (Fr1). The length of basin was obtained according to the calculated conjugate depth (y2) and entrance Froude number (Fr1).

Although the v-notch flow measurement is conducted over a wide range, this experiment will use 10 discharge variations (3.82, 4.34, 4.90, 5.51, 6.15, 6.85, 7.70, 8.36, 9.20, and 10.10) cm3/s. Based on these values, changes in hydraulic characteristics of the stilling basin will be observed. The tailwater height for each discharge value will be calculated using Equation (4) and then set in the flume.

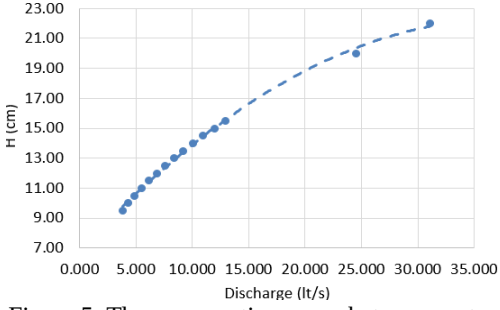

Figure 5. Thompson rating curve between water head elevation (H1) and discharge (Q)

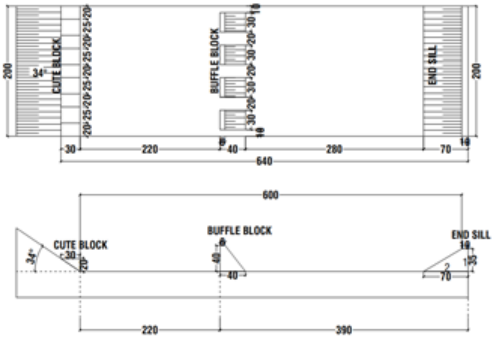

Figure 6. USBR type III stilling basin geometric design results

2.4 Adjusting Tailwater Effect

In the experimental process, each change in discharge also changes the position of the tailwater depth. The tailwater depth height is adjusted from higher to lower until there is no influence from the tailwater depth. The tailwater depth may affect the dissipation effectiveness (ΔE) as a backwater effect. In addition to the parameters in the first variation, the data on tailwater depth height (y3/tw) and damping effectiveness (ΔE) in the second variation were also obtained.

A barrier block using acrylic with the same height as Y2 is used at downstream of the flume to produce the intended tailwater effect. Based on several studies conducted, the condition of the water depth downstream (tailwater depth) greatly affects the effectiveness of dissipation. The shape and dimensions of the barrier block can be seen in Figure 7.

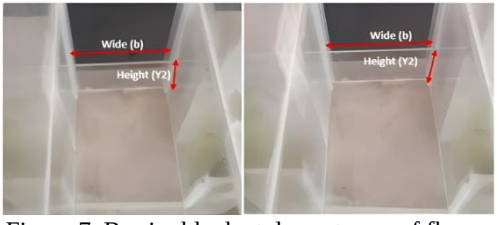

Figure 7. Barrier block at downstream of flume, adjusted from calculated required tailwater depth

Observation of hydraulic parameters due to the influence of tailwater starts from observing the water depth value upstream of the stilling basin (y1) at the toe of the chute channel to the value of water depth downstream of the stilling basin (y2). Documentation of the measurement implementation can be seen in Figure 8.

Figure 8. Measurement of flow depth and velocity over the flume

2.5 Velocity Conditions in Turbulent Area

Velocity testing is conducted in the turbulent area between the chute block and end sill or precisely in the baffle block area. The change in slope from a sharp slope in the launcher channel to a gentle slope in the stilling basin causes the flow to change rapidly, commonly called rapidly varied flow. This condition causes the current conditions to experience turbulence. Irregular patterns, random flow lines, and drastic speed changes characterize this flow. In this test, an automatic speed recording device, the Acoustic Doppler Velocimeter (ADV), produces a velocity recording value. Examples of test documentation at a discharge of 10.1 lt/s can be seen in Figure 9.

Figure 9. Velocity measuerement in turbulent area using ADV

Results and Discussion

Each modeling is tested and obtained data on critical depth (yc), flow velocity along the spillway (v), flow depth (y1) before and after the hydraulic jump (y2), and hydraulic jump length (Lj).

3.1 Results of USBR Type III Model Without Tailwater Effect

Measurement of the critical depth value (yc) was conducted in the launch channel with a pitot pipe tool. The water depth value upstream of the stilling basin (y1) was measured at the foot of the launch channel with manual observation using a ruler. Furthermore, the parameter values of critical depth (yc), Froude Number (Fr), and speed upstream of the stilling basin (v1) and downstream of the stilling basin (v2) were calculated. The graph of the relationship between these parameters can be seen in Fig.10.

Figure 10(a) shows the relationship between the critical depth (yc) that occurs and the flow discharge (Q), where the higher the critical depth water level elevation, the higher the flow discharge.

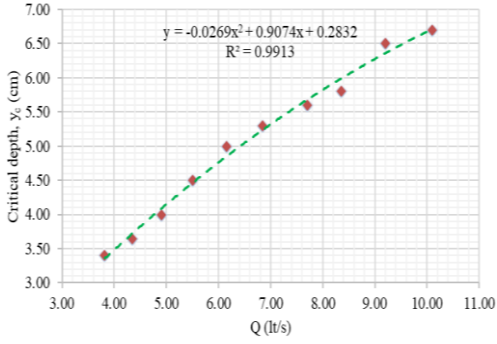

Figure 10(a). Graph between critical depth (yc) and dishcharge (Q)

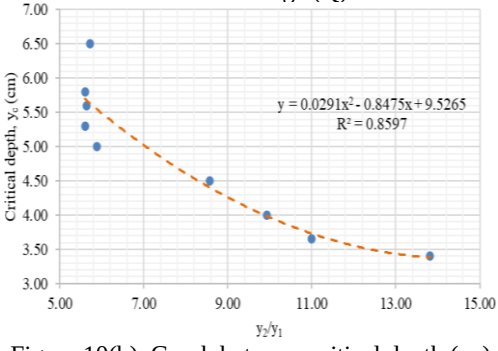

Figure 10(b). Graph between critical depth (yc) and ratio y2/y1

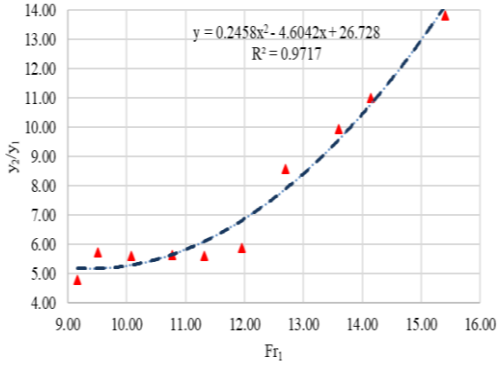

Figure 10(c). Graph between critical depth (yc) and ratio y2/y1

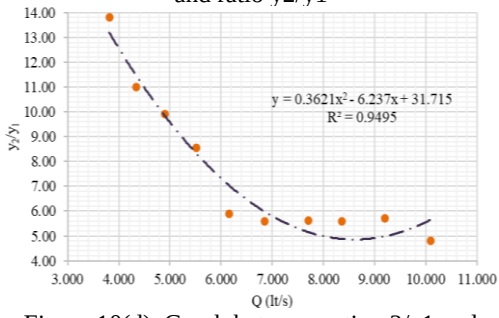

Figure 10(d). Graph between ratio y2/y1 and discharge (Q)

Figure 10(b) shows that the value of yc is inversely proportional to the value of y2/y1, where if the difference in the values of y2 and y1 is greater, the value of yc will be thinner. The comparison of y2/y1 values also affects the resulting Fr1 value, as the graph in Figure 10(c) shows that the higher the difference in y2/y1, the higher the resulting Fr1 value.

Figure 10(d) shows the relationship between flow discharge (Q) and the ratio of y2/y1. The flowing Q value is inversely proportional to the value of the y2/y1 ratio that occurs. The higher the flowing Q value, the smaller the y2/y1 comparison results. This is because the higher the flowing Q, the higher the water level and the smaller the velocity; this causes the hydraulic jump that occurs not to be significant. On the other hand, with a small flowing Q value, the water level that occurs is thin, and the velocity is high, thus causing a high water jump; this causes the difference between y2 and y1 to be higher, which causes supercritical flow.

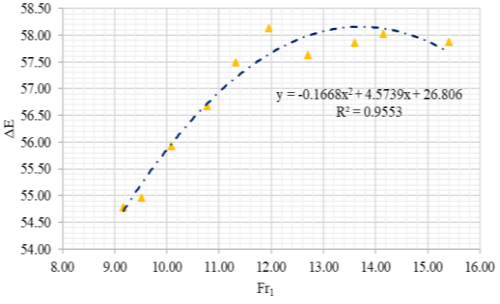

Figure 11(a). Graph between energy loss (ΔE) and Fr1

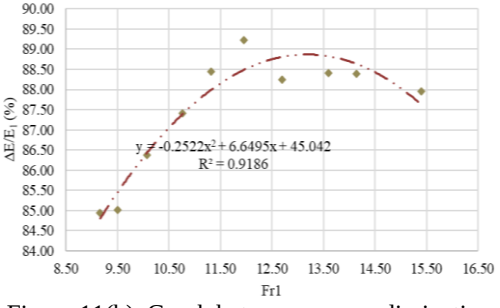

Figure 11(b). Graph between energy dissipation ratio (ΔE/E1) and Fr1

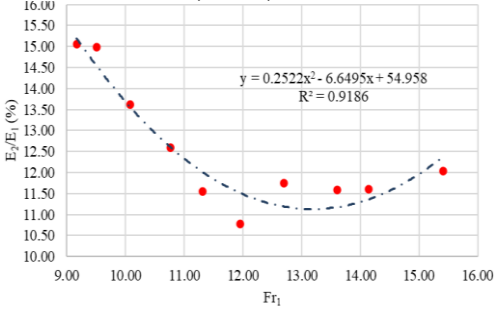

Figure 11(c). Graph between jump efficiency (E2/E1) and Fr1

The following parameters for evaluating the performance of the stilling basin can be measured: energy dissipation ratio (ΔE/E1) and

efficiency (E2/E1). The average energy dissipation ratio of the USBR Type III stilling basin without the influence of tailwater is 87.45%, while the efficiency is 12.55%. A graph of the relationship between efficiency and other parameters is shown in Figure 11.

Figure 11(a) shows the relationship graph between the value of energy loss (ΔE) and Fr1. The higher the energy dissipation that occurs, the higher the FR1 value. The energy dissipation ratio is the ratio between the energy dissipated and the specific energy before the jump (ΔE/E1). The results obtained in Figure 11(b) show that the higher the value of Fr1 that occurs, the higher the energy dissipation ratio. The relative dissipation value will be inversely proportional to the efficiency value, so the graph in Figure 11(c) is opposite to that in Figure 11(b). The greater the relative dissipation value, the smaller the efficiency value of the stilling basin performance, which causes a large Fr1 value. This is because the energy is not ideally dissipated.

3.2 Results of USBR Type III Model with Tailwater Effect

Observation of hydraulic parameters due to the effect of Tailwater starts from observing the water depth value upstream of the stilling basin (y1) at the bottom of the chute channel to the value of water depth downstream of the stilling basin (y2). The average energy dissipation ratio of the USBR Type III Stilling Basin with the influence of Tailwater is 69.47%, while its efficiency is 30.53%. The relationship between parameters is presented in the graphs in Figure 12.

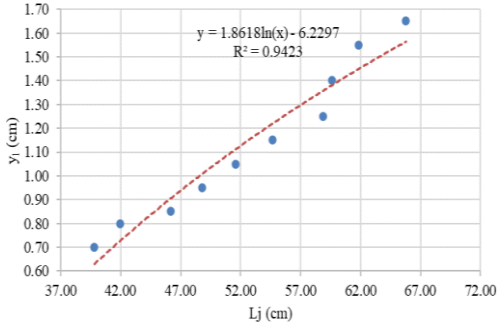

Figure 12(a). Graph between flow depth befor jump (y1) and length of jump (Lj)

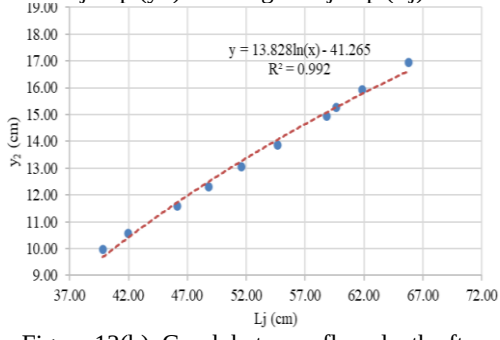

Figure 12(b). Graph between flow depth after jump (y2) and length of jump (Lj)

Figure 12(a) shows the relationship graph between the value of y1 and the hydraulic jump length Lj. It can be seen that the value of y1 is proportional to Lj; the higher the water elevation in y1, the longer the hydraulic jump, as well as the value of y2 shown in Figure 12(b). The difference between the values of y1 and y2 determines the value of the relative energy dissipation. The higher the ratio between y2 and y1, the higher the relative dissipation value, consistent with Figure 12(c).

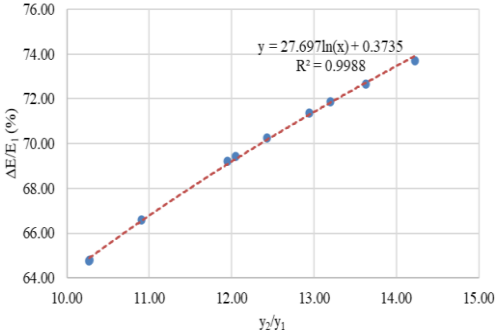

Figure 12(c). Graph between energy dissipation ratio (ΔE/E1) and ratio y2/y1

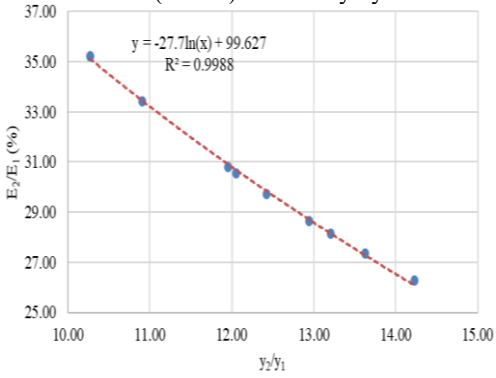

Figure 12(d). Graph between jump efficiency (E2/E1) and ratio y2/y1

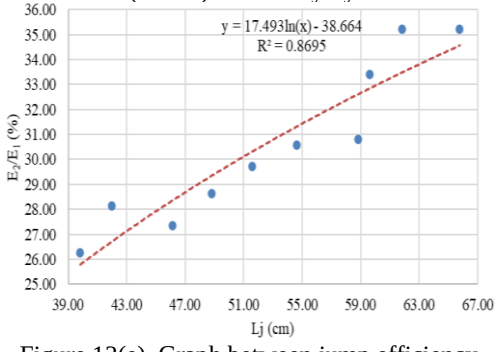

Figure 12(e). Graph between jump efficiency (E2/E1) and length of jump (Lj)

The comparison of y2 and y1 values is inversely proportional to the efficiency; if the values of y2 and y1 are increasingly different, then the efficiency of the performance of the stilling basin will be smaller, as shown in Figure 12(d). Figure 12(e) shows that the longer the hydraulic jump (Lj), the longer the dimension of the stilling basin is needed, causing the efficiency to decrease. It can be interpreted that the value of Lj is inversely proportional to the efficiency value of the stilling.

3.3 Velocity Conditions in Turbulent Areas

The velocity recording resulted from the ADV were conducted in 5 trials. The results of the velocity graph recording, data frequency and average velocity are presented in Figure 13.

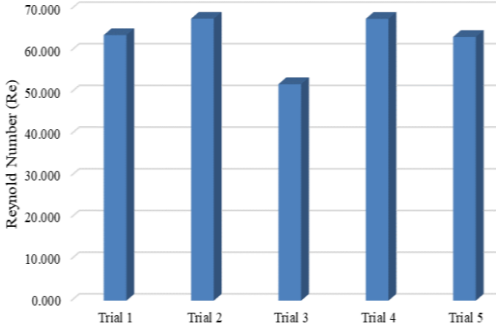

Figure 13. Average velocity (V) in each trial

The average V value in the first trial was 63.689 cm/s, the second trial was 67.629 cm/s, the third trial was 51.923 cm/s, the fourth trial was 67.594 cm/s, and the fifth trial was 63.255 cm/s. Then the average velocity of the five trials conducted was 62.818 cm/s. In actual conditions in the experiment (prototype), the flow conditions at the bottom of the energy dissipator are turbulent. Therefore, in the flume model, the flow conditions at the bottom of the energy dissipator must be turbulent. It can be seen from Reynold's number (Re). The graph of the relationship between hydraulic parameters and Reynold's number (Re) can be seen in Figure 14.

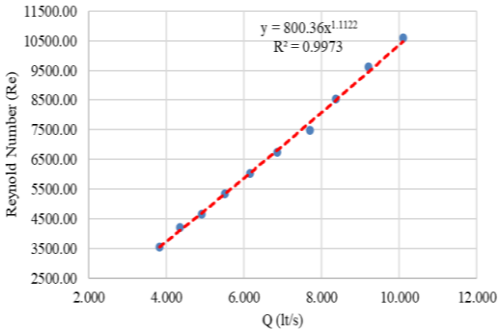

Figure 14(a). Graph between Reynold number (Re) and discharge (Q)

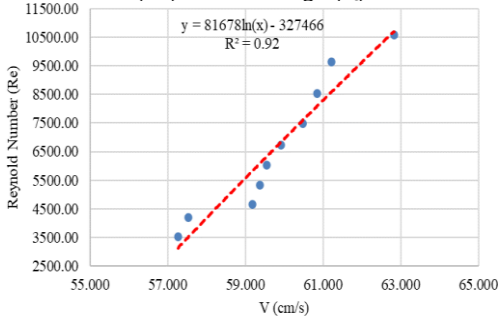

Figure 14(b). Graph between Reynold number (Re) and velocity (V)

The graph in Figure 14(a) shows that the Re value is proportional to the flow discharge. The higher the flow discharge that occurs, the higher the Re value. The higher the velocity, the higher the turbulence value, as shown in Figure 14(b). Figure 14(c) shows that the value of the water level at the time before the hydraulic jump is also proportional to the Re value.

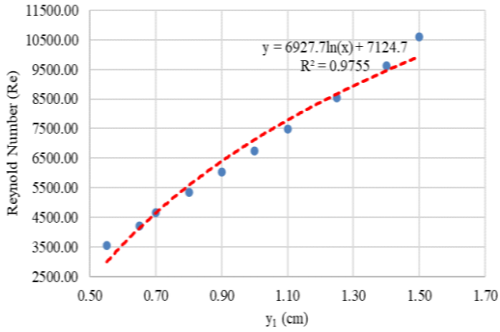

Figure 14(c). Graph between Reynold number (Re) and y1

3.4 Comparison of USBR Type III Prameter Result with and wihout Tailwater Effect

Each hydraulic parameter of the USBR Type III test without the effect of tailwater and with the effect of tailwater can be seen in Figure 15. Figure 15(a) shows that the effect of tailwater causes the performance of the optimum stilling basin because the energy dissipation ratio that occurs is small because the depth of tailwater will help the dissipating value that occurs. The tailwater effect also affects the efficiency value. Figure 15(b) shows that this effect causes the efficiency to be higher than without calculating the effect of Tailwater. The impact of tailwater is that the flow depth value becomes high, causing the velocity to be slower than without tailwater. This can be seen in the graph in Figure 15(c).

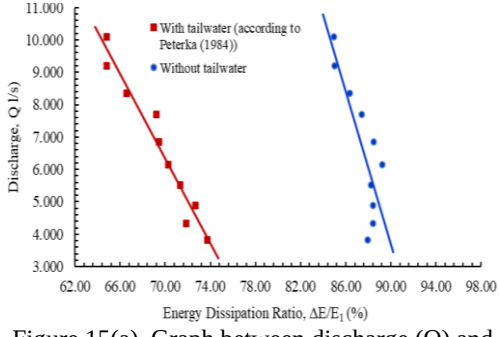

Figure 15(a). Graph between discharge (Q) and energy dissipation ratio (ΔE/E1)

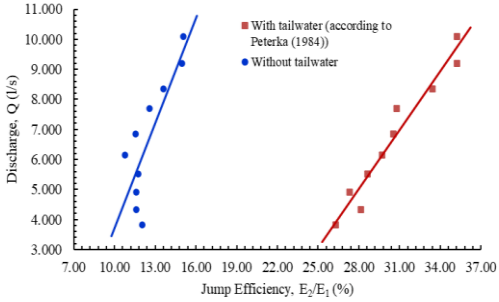

Figure 15(b). Graph between discharge (Q) and jump efficiency (E2/E1)

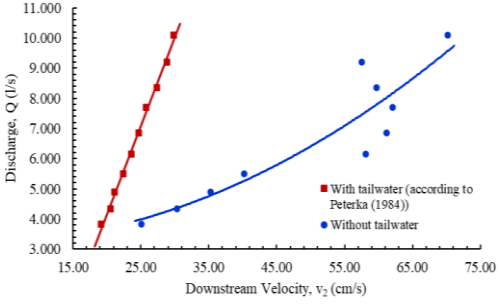

Figure 15(c). Graph between discharge (Q) and downstream velocity (v2)

The water level elevation without tailwater has a lower water level elevation than the water level using tailwater conditions. The y1 condition without Tw is 1.50 cm, and with Tw, it is 1.65 cm. While the value of y2 without Tw is 7.2 cm and with Tw is 16.95 cm, From these conditions, the velocity v2 is 29.80 cm/s if the Froude number at downstream (Fr2) is calculated as follows:

$$Fr_2 = \frac{v_2}{\sqrt{g.y_2}} = \frac{0.2980}{\sqrt{9.81 \times 0.16950}} = 0.22$$

With a Fr2 value of 0.22 (<1), the flow condition with Tw is sub-critical.

Conclusion

Based on this study. The USBR Type III Stilling Basin's performance was assessed under two conditions: without the influence of Tailwater and with the influence of Tailwater. Without Tailwater, the average energy dissipation ratio was found to be 87.45%, resulting in an efficiency of 12.55%. However, when Tailwater was considered, the average energy dissipation ratio decreased to 69.47%, with an efficiency increase to 30.53%. This indicates that the presence of Tailwater significantly impacts the Stilling Basin's performance, enhancing its efficiency. The influence of Tailwater is attributed to its role in reducing the energy dissipation ratio, as the depth of Tailwater facilitates a more effective dissipating process. Additionally, the water level elevation without Tailwater was observed to be lower compared to conditions with Tailwater. Notably, the Froud Numbers (Fr2) value of 0.22 (<1) suggests that the flow condition with tailwater is sub-critical, further emphasizing its positive effect on the stilling basin's performance. With subcritical flow conditions, the velocity in the downstream of the stilling basin will also be smaller. In conclusion, incorporating tailwater in the USBR Type III Stilling Basin design improves its efficiency by optimizing energy dissipation and enhancing flow conditions.

Acknowledgments

The authors would like to thank the Ministry of Education, Culture, Research and Technology (Center for Higher Education Funding-BPPT) and the Lembaga Pengelola Dana Pendidikan (LPDP) for their support in this research.

WORKS CITED

S. Yu et al., 'Geobag stepped spillway for check dams: A pilot study', Int. J. Sediment Res., vol. 38, no. 1, pp. 115–127, 2023, doi: 10.1016/j.ijsrc.2022.07.005.

H. K. Jayant and B. Jhamnani, 'Numerical simulation of free and submerged hydraulic jump over trapezoidal and triangular macroroughness', Heliyon, vol. 9, no. 11, p. e22540, 2023, doi: 10.1016/j.heliyon.2023.e22540.
F. Qin, G. Tao, W. Liu, C. Wu, L. Qi, and J. Li, 'Comparative Study on Energy Dissipation Numerical Simulation of Different Energy Dissipators in Wide and Narrow Alternated Channels', IOP Conf. Ser. Earth Environ. Sci., vol. 526, no. 1, 2020, doi: 10.1088/1755-1315/526/1/012109.
A. Y. Bantacut, A. Azmeri, F. Z. Jemi, Z. Ziana, and M. Muslem, 'An experiment of energy dissipation on USBR IV stilling basin – Alternative in modification', J. Water L. Dev., vol. 53, pp. 68–72, 2022, doi: 10.24425/jwld.2022.140781.
F. Bahmanpouri, C. Gualtieri, and H. Chanson, 'Experiments on two-phase flow in hydraulic jump on pebbled rough bed: Part 2–Bubble clustering', Water Sci. Eng., vol. 16, no. 4, pp. 369–380, 2023, doi: 10.1016/j.wse.2023.05.003.
M. Rubinato, J. Heyworth, and J. Hart, 'Protecting coastlines from flooding in a changing climate: A preliminary experimental study to investigate a sustainable approach', Water (Switzerland), vol. 12, no. 9, 2020, doi: 10.3390/w12092471.
A. Javed, K. F. Khan, M. A. Quasim, and S. Asjad, 'Diagenetic characteristics and their implications on the reservoir potential of Bajocian Sandstone, Jaisalmer Basin, western Rajasthan, India', Geosystems and Geoenvironment, vol. 2, no. 4, 2023, doi: 10.1016/j.geogeo.2023.100219.
J. Huang, R. Li, J. Feng, Z. Li, X. Cheng, and Z. Wang, 'The Application of Baffle Block in Mitigating TDGS of Dams with Different Discharge Patterns', Ecol. Indic., vol. 133, 2021, doi: 10.1016/j.ecolind.2021.108418.
L. Kong, L. Ma, Y. Li, J. Abuduwaili, and J. Zhang, 'Assessing the intensity of the water cycle utilizing a Bayesian estimator algorithm and wavelet coherence analysis in the Issyk-Kul Basin of Central Asia', J. Hydrol. Reg. Stud., vol. 52, no. August 2023, p. 101680, 2024, doi: 10.1016/j.ejrh.2024.101680.
W. H. M. Wan Mohtar et al., 'Assessment of dam appurtenant structures under multiple flow discharge scenarios', Ain Shams Eng. J., vol. 11, no. 4, pp. 913–922, 2020, doi: 10.1016/j.asej.2020.03.009.
J. F. Macián-Pérez, R. García-Bartual, B. Huber, A. Bayon, and F. J. Vallés-Morán, 'Analysis of the flow in a typified USBR II stilling basin through a numerical and physical modeling approach', Water (Switzerland), vol. 12, no. 1, 2020, doi: 10.3390/w12010227.
S. Y. Kumcu and K. Ispir, 'Experimental and numerical modeling of various energy dissipater designs in chute channels', Appl. Water Sci., vol. 12, no. 12, pp. 1–15, 2022, doi: 10.1007/s13201-022-01792-3.
Z. M. Yan, C. T. Zhou, and S. Q. Lu, 'Pressure fluctuations beneath spatial hydraulic jumps', J. Hydrodyn., vol. 18, no. 6, pp. 723–726, 2006, doi: 10.1016/S1001-6058(07)60012-2.
T. Masuda, T. Tagawa, M. M. A. Alam, and Y. Hayamizu, 'Structure of Periodic Flows through a Channel with a Suddenly Expanded and Contracted Part', Open J. Fluid Dyn., vol. 13, no. 05, pp. 232–249, 2023, doi: 10.4236/ojfd.2023.135018.
A. B. A. Sakarya and N. D. Tokyay, 'Numerical simulation of A-type hydraulic jumps at positive steps', Can. J. Civ. Eng., vol. 27, no. 4, pp. 805–813, 2000, doi: 10.1139/cjce-27-4-805.
C. D. Svoboda, R. F. Einhellig, and K. W. Frizell, 'Hydraulic Model Study of Folsom Dam Joint Federal Project Auxiliary Spillway Confluence Area', no. February, 2010, [Online]. Available: http://www.ntis.gov
M. W. Zaffar et al., 'Numerical investigation of hydraulic jumps with USBR and wedge-shaped baffle block basins for lower tailwater', Aqua Water Infrastructure, Ecosyst. Soc., vol. 72, no. 0, pp. 2081–2108, 2023, doi: 10.2166/aqua.2023.261.
N. D. Tokyay, T. U. Evcimen, and C. Şimşek, 'Forced hydraulic jump on non-protruding rough beds', Can. J. Civ. Eng., vol. 38, no. 10, pp. 1136–1144, 2011, doi: 10.1139/l11-072.
V. H. Vayghan, M. Mohammadi, and A. Ranjbar, 'Experimental Study of the Rooster Tail Jump and End Sill in Horseshoe Spillways', Civ. Eng. J., vol. 5, no. 4, pp. 871–880, 2019, doi: 10.28991/cej-2019-03091295.
H. L. Tiwari and A. Goel, 'Effect of End Sill in the Performance of Stilling Basin Models', Am. J. Civ. Eng. Archit., vol. 2, no. 2, pp. 60–63, 2014, doi: 10.12691/ajcea-2-2-1.
M. M. Ibrahim, M. A. Refaie, and A. M. Ibraheem, 'Flow characteristics downstream stepped back weir with bed water jets', Ain Shams Eng. J., vol. 13, no. 2, p. 101558, 2022, doi: 10.1016/j.asej.2021.08.003.
E. A. Elnikhely and I. Fathy, 'Prediction of scour downstream of triangular labyrinth weirs', Alexandria Eng. J., vol. 59, no. 2, pp. 1037–1047, 2020, doi: 10.1016/j.aej.2020.03.025.

E. Gül, Z. Kılıç, E. İkincioğulları, and M. C. Aydın, 'Investigation of the effect of variable-sized energy dissipating blocks on sluice gate performance', Water SA, vol. 50, no. 1, pp. 92–105, 2024, doi: 10.17159/wsa/2024.v50.i1.4064.
Y. Zhou, J. Wu, H. Zhao, J. Hu, and F. Bai, 'Hydraulic Performance of Wave-Type Flow at a Sill-Controlled Stilling Basin', Appl. Sci., vol. 13, no. 8, 2023, doi: 10.3390/app13085053.
T. L. Wahl and H. T. Falvey, 'SpillwayPro: Integrated Water Surface Profile, Cavitation, and Aerated Flow Analysis for Smooth and Stepped Chutes', Water (Switzerland), vol. 14, no. 8, 2022, doi: 10.3390/w14081256.
M. Gebhardt, U. Pfrommer, T. Rudolph, and C. Thorenz, 'Numerical and physical study on the energy dissipation at inflatable gates', 7th IAHR Int. Symp. Hydraul. Struct. ISHS 2018, vol. 26, pp. 174–183, 2018, doi: 10.15142/T3JD26.
N. Hassanpour, A. H. Dalir, A. Bayon, and M. Abdollahpour, 'Pressure fluctuations in the spatial hydraulic jump in stilling basins with different expansion ratio', Water (Switzerland), vol. 13, no. 1, pp. 1–15, 2021, doi: 10.3390/w13010060.
S. Soori, H. Babaali, and N. Soori, 'An Optimal Design of the Inlet and Outlet Obstacles at USBR II Stilling Basin', Int. J. Sci. Eng. Appl., vol. 6, no. 5, pp. 134–142, 2017, doi: 10.7753/ijsea0606.1001.
R. R. Bhate, M. R. Bhajantri, and V. V. Bhosekar, 'Mitigating cavitation on high head orifice spillways', ISH J. Hydraul. Eng., vol. 27, no. 3, pp. 235–243, 2021, doi: 10.1080/09715010.2018.1547990.
E. JG and A. JC, 'The proposed modeling and experimental design of a test section of a hydraulic jump in an open flow channel The proposed modeling and experimental design of a test section of a hydraulic jump in an open flow channel', Eur. J. Adv. Eng. Technol., no. February, 2021, doi: 10.13140/RG.2.2.23362.91848.
N. Torkamanzad, A. H. Dalir, F. Salmasi, and A. Abbaspour, 'Hydraulic jump below abrupt asymmetric expanding stilling basin on rough bed', Water (Switzerland), vol. 11, no. 9, pp. 1–29, 2019, doi: 10.3390/w11091756.
D. Demiral, R. M. Boes, and I. Albayrak, 'Effects of secondary currents on turbulence characteristics of supercritical open channel flows at low aspect ratios', Water (Switzerland), vol. 12, no. 11, pp. 1–24, 2020, doi: 10.3390/w12113233.
V. Dermawan, Suhardjono, L. Prasetyorini, and S. Anam, 'Hydraulic model experiment of energy dissipation on the horizontal and USBR II stilling basin', IOP Conf. Ser. Earth Environ. Sci., vol. 930, no. 1, 2021, doi: 10.1088/1755-1315/930/1/012029.
S. M. Formentin, G. Palma, and B. Zanuttigh, 'Integrated assessment of the hydraulic and structural performance of crown walls on top of smooth berms', Coast. Eng., vol. 168, no. June, p. 103951, 2021, doi: 10.1016/j.coastaleng.2021.103951.
J. N. Bradley and A. J. Peterka, 'Hydraulic Design of Stilling Basins: Hydraulic Jumps on a Horizontal Apron (Basin I)', J. Hydraul. Div., vol. 83, no. 5, 1957, doi: https://doi.org/10.1061/jyceaj.0000126.
A. J. Peterka, Hydraulic Design of Stilling Basins and Energy Dissipators, vol. 25. Denver, Colorado: United States Department of Interior Bureau Reclamation, 1984. doi: 10.1061/jyceaj.0000243.